Biochemical and Biophysical Research Communications 425 (2012) 374–378

Contents lists available at SciVerse ScienceDirect

Biochemical and Biophysical Research Communications

journal homepage: www.elsevier.com/locate/ybbrc

Pyrite footprinting of RNA

Jörg C. Schlatterer [a,*], Matthew S. Wieder [a], Christopher D. Jones [b], Lois Pollack [b], Michael Brenowitz [a]

[a] Department of Biochemistry, Albert Einstein College of Medicine, Bronx, NY, USA
[b] School of Applied and Engineering Physics, Cornell University, Ithaca, NY, USA

ARTICLE INFO

Article history:
Received 17 July 2012
Available online 27 July 2012

Keywords:
Pyrite
RNA
Hydroxyl radical
Footprinting

ABSTRACT

In RNA, function follows form. Mapping the surface of RNA molecules with chemical and enzymatic probes has revealed invaluable information about structure and folding. Hydroxyl radicals (·OH) map the surface of nucleic acids by cutting the backbone where it is accessible to solvent. Recent studies showed that a microfluidic chip containing pyrite (FeS_2) can produce sufficient ·OH to footprint DNA. The 49-nt Diels–Alder RNA enzyme catalyzes the C–C bond formation between a diene and a dienophile. A crystal structure, molecular dynamics simulation and atomic mutagenesis studies suggest that nucleotides of an asymmetric bulge participate in the dynamic architecture of the ribozyme's active center. Of note is that residue U42 directly interacts with the product in the crystallized RNA/product complex. Here, we use powdered pyrite held in a commercially available cartridge to footprint the Diels–Alderase ribozyme with single nucleotide resolution. Residues C39 to U42 are more reactive to ·OH than predicted by the solvent accessibility calculated from the crystal structure suggesting that this loop is dynamic in solution. The loop's flexibility may contribute to substrate recruitment and product release. Our implementation of pyrite-mediated ·OH footprinting is a readily accessible approach to gleaning information about the architecture of small RNA molecules.

1. Introduction

RNA is at the heart of the central dogma of biology [1]. Since the biological function of RNA is often dependent on its three dimensional structure, the development of new methods of structure determination can provide insight into the modulation of biological processes by RNA. Crystallography and NMR can be used to reveal atomic resolution structures but are costly to apply to RNA in both time and funds. Chemical mapping ('footprinting') of RNA can provide structural insight by quantifying the reactivity of the macromolecule to an exogenous probe with as fine as single nucleotide resolution [2–5]. The high reactivity, small size, and sequence independency of the hydroxyl radical (·OH) has made this probe invaluable for revealing RNA structure, binding interfaces and dynamics [3,6–8]. Hydroxyl radical footprinting has been recently used as an experimental constraint for modeling RNA structure [9].

We recently demonstrated that powdered pyrite (FeS_2) can serve as a solid matrix for ·OH production in sufficient quantities to footprint DNA for structural analysis [10]. Herein, we apply this approach to RNA by analyzing the 49-nucleotide Diels–Alderase ribozyme. The *in vitro* evolved Diels–Alderase ribozyme catalyzes the [4 + 2] cyclo-addition reaction between a diene and a dienophile [11]. This ribozyme is the first *in vitro* selected nucleic acid to accelerate a cycloaddition reaction in a truly bimolecular fashion and with high enantioselectivity [12,13]. Crystallographic analysis revealed a discrete three-dimensional structure whose catalytic core is a tight nucleotide network involving residues from the asymmetric bulge and the 5′ terminus [14]. While the mechanism by which the ribozyme mediates substrate recruitment and product release is unknown, it is likely that catalysis relies on flexibility and solvent accessibility of stretches of nucleotides around the catalytic core.

In this work, we use powdered pyrite housed in a commercially available cartridge to map the solvent accessible surface of the Diels–Alderase ribozyme with single nucleotide resolution. The dose of ·OH to which the RNA was exposed is readily and accurately controlled by solution flow rate such that single hit kinetic cleavage is achieved. The ·OH reactivity profiles of the ribozyme are comparable with those derived from the standard Fe-EDTA footprinting method [7]. Comparison with the calculated solvent accessible surface area of crystal structure (1YKQ) of the free Diels–Alderase suggests that CAAU, located in the asymmetric bulge, is more solvent accessible in solution than in the crystal and may thus be a dynamic participant in the postulated kick-in/kick-off mechanism for substrate recruitment and product release [15].

* Corresponding author. Address: Department of Biochemistry, Albert Einstein College of Medicine, 1300 Morris Park Ave., Bronx, NY 10461, USA. Fax: +1 718 430 8565.
E-mail address: joerg.schlatterer@einstein.yu.edu (J.C. Schlatterer).

0006-291X/$ - see front matter © 2012 Elsevier Inc. All rights reserved.
http://dx.doi.org/10.1016/j.bbrc.2012.07.100

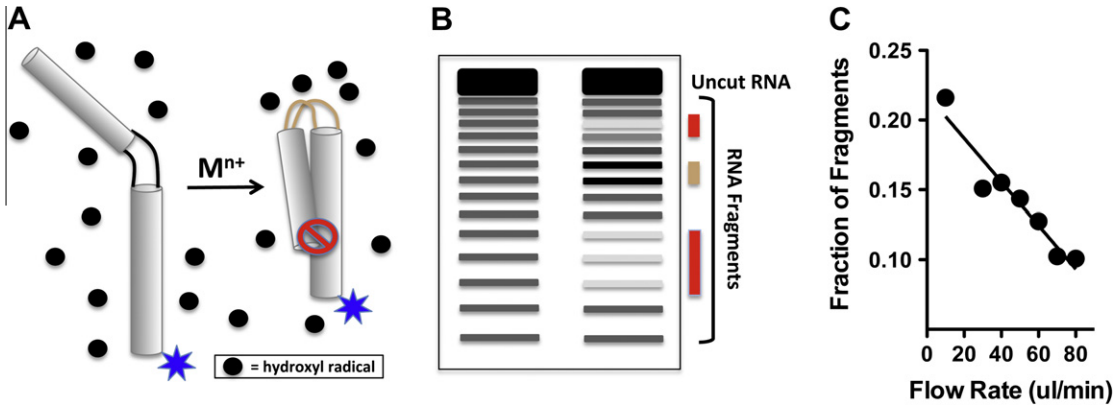

Fig. 1. (A) Scheme of metal ion mediated tertiary structure formation of P4–P6 RNA. The unfolded (left) and folded (right) RNA is exposed to hydroxyl radicals (black dots). Upon folding some nucleotides become more protected (red circle) from the attack of ·OH, some nucleotides become more accessible (light red hinge) to hydroxyl radicals. The blue stars indicate a radioactive label at the 5′ end of the RNA. (B) Sequencing gel cartoon displaying ·OH footprinted unfolded (left) and folded (right) RNA samples. The lighter the RNA fragment bands are the more protected is the corresponding nucleotide against the attack of hydroxyl radicals. The dark and light red bars correspond to protected and exposed nucleotides in (A), respectively. (C) P4–P6 RNA fragmentation as function of flow rate using a pyrite filled microfluidic chip [10], unpublished data. Varying flow rates between 10 and 80 μL/min results in relative fragmentation of RNA between 22% and 9%, respectively. Flow rates above 10 μL/min are consistent with single hit kinetics conditions [17] and can be used for footprinting. (For interpretation of the references to colour in this figure legend, the reader is referred to the web version of this article.)

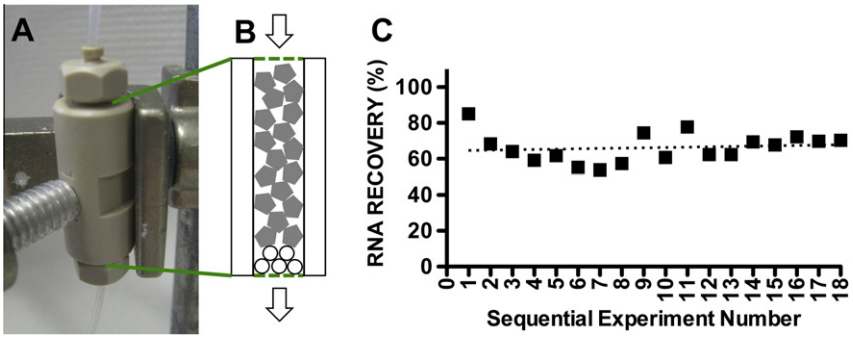

Fig. 2. Pyrite footprinting using a commercially available cartridge. (A) Picture of the 10 μL CapTide cartridge. (B) Filling scheme of the CapTide cartridge. Pyrite particles (63–180 μm) are layered above glass beads (200–300 μm). (C) The RNA recovery rate is projected over the experimental time line.

2. Materials and methods

2.1. RNA sample preparation

T7 RNA polymerase *in vitro* transcription of PCR-generated DNA templates containing wild-type ribozyme generated the P4–P6 RNA domain of the Tetrahymena ribozyme. Transcribed P4–P6 RNA is gel purified prior to ^{32}P labeling. The 49-nucleotide Diels–Alderase ribozyme was synthesized by phosphoramidite chemistry at Almac Sciences. RNA was radiolabeled at the 5′ end with [**γ-**^{32}P] ATP as described [16]. The ^{32}P RNA was dissolved in 1 mM sodium cacodylate buffer (pH 7.4), stored at −20 °C and used within two days after labeling. Five micromolars of RNA in 1 mM sodium cacodylate buffer were denatured by heating to 90 °C for 1 min, then cooled on ice and incubated at 25 °C prior to metal ion addition and footprinting.

2.2. Preparation of pyrite particles and cartridge

Approximately 17 g of ground pyrite with a particle size distribution of 63–180 μm is obtained from 100 g of raw mineral as previously described [10]. A 10 μL CapTide refillable cartridge (uCTG-10-360) was purchased from Labsmith (Livermore, CA 94551) secured as shown in Fig. 2A for pyrite loading and experimental studies. Ten microns of polyethylene mesh affixed to a screw cap is placed at the bottom of the cartridge on top of which is added 2–3 μL of glass beads (200–300 μm). About 20 mg of the powdered pyrite is suspended in 0.5 mL of nanopure deionized water. The cartridge is filled with the pyrite slurry pulling the solution with a gentle vacuum. The top of the cartridge is sealed with a second mesh covered screw cap as per the manufacturers instruction. The pyrite is activated by flushing with 5 mL of HCl (0.5 M) at a flow rate of 100 μL/min. The pyrite is then flushed with 5 mL of degassed, DEPC treated water (AMBION) at a flow rate of 100 μL/min until the pH of the eluent is ∼4.5. Pyrite is reactivated by acid treatment daily or after 20–25 footprinting experiments.

2.3. Pyrite footprinting of RNA

^{32}P-labeled ribozyme was equilibrated at the indicated metal ion concentrations for 30 min at room temperature prior to footprinting. H_2O_2 was added at the indicated concentration before the samples are loaded into the inlet tube. The pumped drive syringe (Harvard Apparatus), contains degassed, DEPC treated water (AMBION). ^{32}P-RNA samples of 30 μL are footprinted by flowing the sample flanked by 10–20 μL air bubbles through the cartridge at a constant flow rate and into a microfuge tube containing 300 μL absolute ethanol. Cerenkov counting prior to processing of the samples quantitates the relative amount of ^{32}P-RNA recovery.

The ^{32}P-RNA is then precipitated by immersion of the tube in a dry ice ethanol bath and the reaction products separated, imaged and quantitated as described elsewhere [7,10,17]. Due to the small

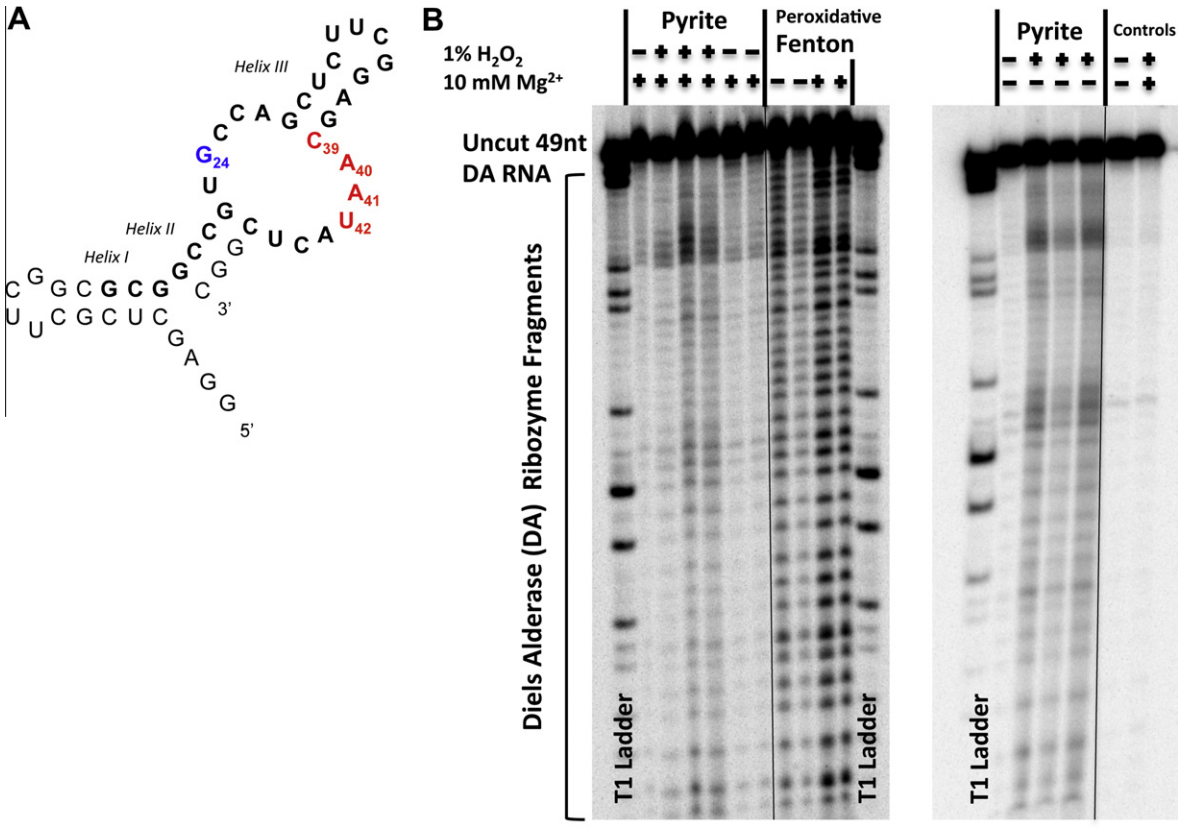

Fig. 3. Pyrite facilitated hydroxyl radical footprinting of the Diels–Alderase ribozyme. (A) Secondary structure of the Diels–Alderase minimal motif. Footprinting studies employed the 49-nucleotide RNA whereas the discussed crystal structure was derived from a catalytically active, bi-partite RNA molecule. (B) Representative sequencing gels of ·OH footprinted DA RNA samples at +/−10 mM Mg(II) and 1% H_2O_2, respectively.

length of the RNA, the ·OH cleavage products of the Diels–Alderase ribozyme were separated using a 15% denaturing polyacrylamide gel and overnight exposure of the wet gel to a storage phosphor screen at 4 °C. The quantitated band intensities were internally normalized to facilitate comparison among the data sets. All experiments were repeated three times.

The solvent accessible surface area of the Diels–Alderase ribozyme was calculated using GETAREA to analyze the atomic coordinates from pdb file 1YKQ [14] with a probe radius of 1.4 Å [18]. The corresponding nucleotide range was internally normalized to facilitate comparison with the ·OH reactivity profiles.

2.4. Peroxidative Fe-EDTA footprinting

Peroxidative Fe-EDTA footprinting is performed at room temperature following standard protocols as described elsewhere [7] and analyzed as described above for the pyrite footprinted samples.

3. Results and discussion

Hydroxyl radical footprinting is a well established method for determining the structure and folding of RNA molecules and their complexes [19,20]. Fig. 1A summarizes the RNA footprinting experiment [7,17]. End-labeled RNA is exposed to a dose of ·OH such that on average every molecule is cut only once ('single hit kinetics') [21]. Experiments are often conducted as a function of a variable such as cation type and/or concentration that affects folding or complex formation. The ·OH will cleave the phosphodiester backbone where it is accessible to the solvent. Colloquially, ·OH determines which backbone positions are inside and which are outside with single nucleotide resolution [22]. The cleavage sites are detected by sorting the reaction products by size, typically with polyacrylamide electrophoresis and quantitated by phosphor storage imaging; dark bands reflect accessible residues while lighter bands reflect residues that are protected from solvent. We have shown that single-hit cleavage kinetics can be achieved with DNA [10] and RNA (Fig. 1C) by controlling the rate that the nucleic acid containing solution flows through activated pyrite.

The microfluidic device used in our published study is the foundation for pyrite footprinting devices [10]. Here we use a commercially available cartridge for RNA structure mapping. A layer of glass beads is laid above the bottom mesh of the 10 μL CapTide cartridge and then gently filled with pyrite ground and sieved to 63–180 μm particles (Fig. 2). This configuration results in stable fluid flow over tens of experimental replicates (data not shown). Reproducible recovery of 60–70% of the RNA was obtained (Fig. 2C). The 'lost' RNA is absorbed to the pyrite surface consistent with electrostatic interactions of the mineral surface with nucleic acids [23]. The absorbed RNA is cleaned from the mineral after an experiment by acid washing.

The secondary structure of the Diels–Alderase ribozyme features three helices (I–III) and an asymmetric bulge (Fig. 3A). Solution of its three dimensional structure was accomplished by utilizing a bi-partite RNA complex without the closing tetra-loop of helix I of the original 49-nt RNA and an A → G mutation of nucleotide 27 [14]. The product complexes of the ribozyme and the free Diels–Alderase RNA show identical λ-shaped architecture with collinear stacking of helices II and III and a bridging asymmetric bubble [14]. While Mg^{2+} is necessary to form a catalytically active structure it does not directly participate in catalysis [11,12,24].

An imino proton NMR spectra shows that the majority of the Diels–Alderase structure is formed when the ratio of RNA to Mg(II) is 1:2 [14].

The Diels–Alderase ribozyme is active over a wide range of solution conditions, 30–300 mM NaCl and 10–80 mM $MgCl_2$ [12,25]. Single-molecule FRET and solution NMR studies indicate that the Diels–Alderase ribozyme is highly dynamic at room temperature [26,27]. Atomic mutagenesis studies suggest that catalytically active RNA relies on the interaction of U42 with G24 and $[Mg(H_2O)_6]^{2+}$ and that, for efficient catalysis, the ribozyme demands a sensitive equilibrium between rigidity and flexibility [25]. We ask in this study is whether pyrite-mediated ·OH footprinting can be used to probe the structure and flexibility of a functional RNA molecule identifying nucleotides potentially involved in substrate recruitment and product release.

Robust pyrite-mediated ·OH cleavage of the ^{32}P-labeled Diels–Alderase ribozyme was obtained under the experimental conditions utilized in this study. The expected single nucleotide resolution and fragmentation comparable to Fe-EDTA footprinting is evident in Fig. 3B. Negligible degradation of the RNA is observed for samples passed through the cartridge in the absence of H_2O_2, consistent with previous results [10]. Comparable ·OH cleavage was observed in 50 mM NaCl and Mg(II) up to 10 mM (Fig. 4A). Pyrite is a suitable solid substrate for ·OH footprinting of RNA.

Quantitation of the extent of each nucleotide's cleavage reveals consistent profiles for pyrite-mediated and Fe-EDTA-mediated ·OH footprinting (Fig. 4A, lower two panels). The ·OH cleavage profiles are consistent with the solvent accessible surface calculated from the crystal structure with one significant exception (Fig. 4A, top three panels). The exception is the enhanced ·OH reactivity of the nucleotides C39–U42 involved in helix III and asymmetric bulge formation; these nucleotides are more reactive than the solvent accessibility calculated from the structure (Figs. 3A and 4A, red). The presence of NaCl in the presence of $MgCl_2$ does not significantly change the ·OH cleavage profile (Fig. 4A, panels two and three). This result is expected as Mg^{2+} effectively stabilizes RNA tertiary structure at low concentrations.

Nucleotides C39–U42 form the roof of the catalytic pocket. U42 participates in the base triple U42· (G2–C25). G24 is sandwiched between U23 and U42. Stacking interactions of the nucleotide 27 – A40 pair, A41· (G1–C26) three base platform and U42· (G2–C25) define the complex structure of the catalytic core [14]. The 2′ OH of U42 forms a hydrogen bond with one of the carbonyl oxygens of the maleimide derivative in the ribozyme product complex. Catalytic activity strongly depends on the interaction of U42 with G24 [25]. A magnesium ion interacts with both of these nucleotides (Fig. 4B, dashed lines) [14]. Molecular dynamics (MD) simulation studies suggest that the catalytic pocket of the Diels–Alderase ribozyme is highly dynamic, fluctuating between an open (active) and a closed (inactive) state [28]. The tetraloop nucleotides of helices I and III are most flexible, followed by nucleotides C39–U42 [29].

The increased ·OH reactivity of residues C39–U42 indicates that these nucleotides are more solvent accessible than indicated by the crystal structure and that this dynamic behavior may play a significant role in the structure and function of the Diels–Alderase RNA. This finding is consistent with the versatile responsibilities of C39–U42 in the architecture of the catalytic pocket, confirming a substantial role in the mechanism by which the ribozyme performs catalysis. Flexibility of this region might be important in recruiting of the maleimide compound, formation of the active center, stabilization of the transition state, and product release. These findings suggest that detailed studies assessing the solvent accessibility and flexibility of the asymmetric bubble of the Diels–Alder RNA at different solution conditions and in the presence of substrates or products might help unravel the conformational changes that underlie the catalysis activity of this ribozyme.

Taken together, these data support the hypothesis that structural information about small RNA enzymes can be obtained by pyrite-mediated ·OH footprinting. Using inexpensive mineral, a

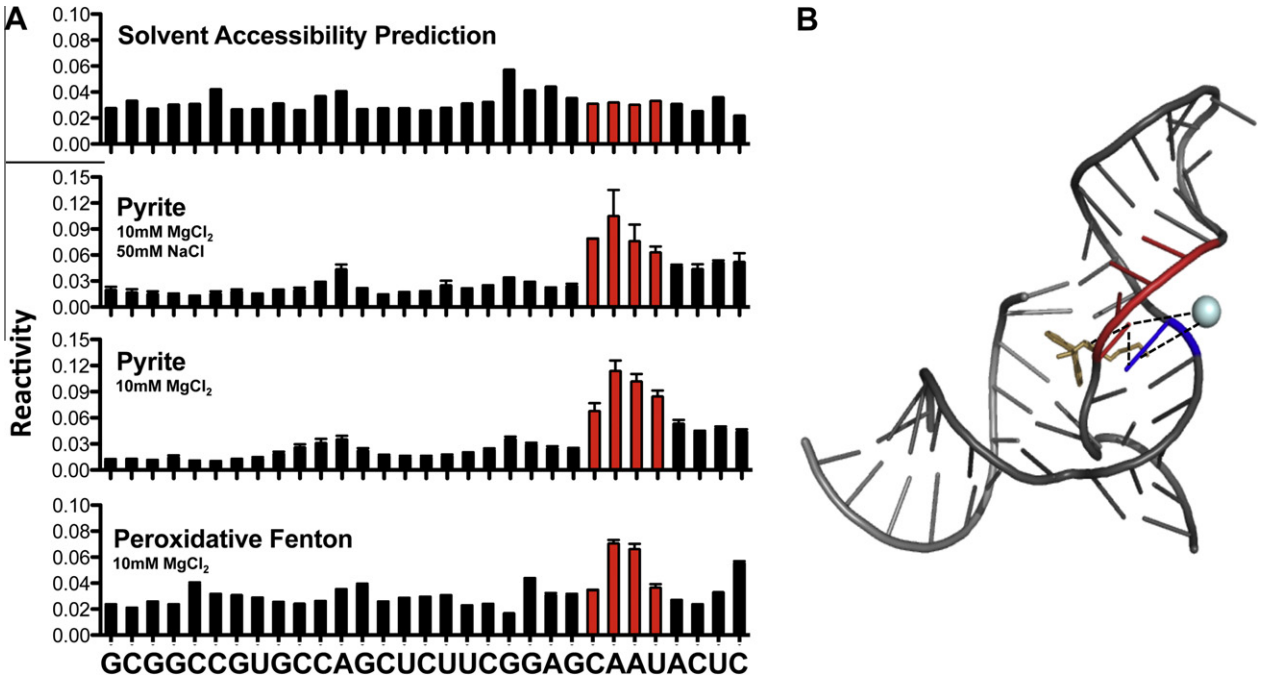

Fig. 4. (A) Profiles of solvent accessible surface area (SASA) of the Diels–Alderase derived from traditional Fenton (bottom) and pyrite (two middle panels) technology. The top panel shows the predicted SASA derived from the protein data base archived crystal structure (1YKQ). Red nucleotides indicate a significant difference between predicted and experimental data. (B) Three-dimensional representation of the Diels–Alderase ribozyme – product complex (1YLS). The reaction product between N-pentylmaleimide and 9-hydroxymethylanthracence is shown in yellow. Interactions between U_{42} (red) and G_{24} (blue), the maleimide compound of the reaction product and Mg^{2+} are shown as dashed lines. (For interpretation of the references to colour in this figure legend, the reader is referred to the web version of this article.)

commercially available cartridge and the Diels–Alderase ribozyme, we mapped the RNA backbone reactivity towards ·OH. The pyrite method is well suited to repetitive measurements such as required for scanning or high-throughput analyses. We showed that results of pyrite footprinting experiments are consistent with the conventional Fe-EDTA method. Hydroxyl radical footprinting can add value to structural studies of small RNAs such as ribozymes and aptamers by revealing accessibility and flexibility of nucleotides that might adopt a crucial role in the RNA's function.

Acknowledgments

We thank Dr. Andres Jäschke (IPMB, University of Heidelberg) for donating the Diels–Alderase RNA. Matthew Wieder was a participant in and supported by the Einstein Summer Undergraduate Research Program (SURP). We thank Madeline Finkelstein (Cornell University) for assistance in assembling microfluidic devices. This work was supported by the NSF through the IDBR program (0852796 and 0852813).

References

[1] G.F. Joyce, The antiquity of RNA-based evolution, Nature 418 (2002) 214–221.
[2] T.D. Tullius, B.A. Dombroski, Iron(II) EDTA used to measure the helical twist along any DNA molecule, Science 230 (1985) 679–681.
[3] T.D. Tullius, B.A. Dombroski, Hydroxyl radical "footprinting": high-resolution information about DNA-protein contacts and application to lambda repressor and Cro protein, Proc. Natl. Acad. Sci. USA 83 (1986) 5469–5473.
[4] T.D. Tullius, B.A. Dombroski, M.E. Churchill, L. Kam, Hydroxyl radical footprinting: a high-resolution method for mapping protein-DNA contacts, Methods Enzymol. 155 (1987) 537–558.
[5] J.A. Latham, T.R. Cech, Defining the inside and outside of a catalytic RNA molecule, Science 245 (1989) 276–282.
[6] B. Sclavi, M. Sullivan, M.R. Chance, M. Brenowitz, S.A. Woodson, RNA folding at millisecond intervals by synchrotron hydroxyl radical footprinting, Science 279 (1998) 1940–1943.
[7] R. Bachu, F.C. Padlan, S. Rouhanifard, M. Brenowitz, J.R. Schlatterer, Monitoringequilibrium changes in RNA structure by 'Peroxidative' and 'Oxidative' hydroxyl radical footprinting, J. Vis. Exp. 56 (2011) e3244, http://dx.doi.org/10.3791/3244.
[8] D.W. Celander, T.R. Cech, Iron(II)-ethylenediaminetetraacetic acid catalyzed cleavage of RNA and DNA oligonucleotides: similar reactivity toward single- and double-stranded forms, Biochemistry 29 (1990) 1355–1361.
[9] F. Ding, C.A. Lavender, K.M. Weeks, N.V. Dokholyan, Three-dimensional RNA structure refinement by hydroxyl radical probing, Nat. Methods 9 (2012) 603–608.
[10] C.D. Jones, J.C. Schlatterer, M. Brenowitz, L. Pollack, A microfluidic device that generates hydroxyl radicals to probe the solvent accessible surface of nucleic acids, Lab Chip 11 (2011) 3458–3464.
[11] B. Seelig, A. Jaschke, A small catalytic RNA motif with Diels–Alderase activity, Chem. Biol. 6 (1999) 167–176.
[12] B. Seelig, S. Keiper, F. Stuhlmann, A. Jaschke, Enantioselective ribozyme catalysis of a bimolecular cycloaddition reaction, Angew. Chem. Int. Ed. Engl. 39 (2000) 4576–4579.
[13] J.C. Schlatterer, F. Stuhlmann, A. Jaschke, Stereoselective synthesis using immobilized Diels–Alderase ribozymes, ChemBioChem 4 (2003) 1089–1092.
[14] A. Serganov, S. Keiper, L. Malinina, V. Tereshko, E. Skripkin, C. Hobartner, A. Polonskaia, A.T. Phan, R. Wombacher, R. Micura, Z. Dauter, A. Jaschke, D.J. Patel, Structural basis for Diels–Alder ribozyme-catalyzed carbon–carbon bond formation, Nat. Struct. Mol. Biol. 12 (2005) 218–224.
[15] J.C. Schlatterer, Funtionalized Nucleic Acids: Studies & Selection of Ribozymes, University of Heidelberg, Heidelberg, 2003.
[16] A.J. Zaug, C.A. Grosshans, T.R. Cech, Sequence-specific endoribonuclease activity of the tetrahymena ribozyme: enhanced cleavage of certain oligonucleotide substrates that form mismatched ribozyme-substrate complexes, Biochemistry 27 (1988) 8924–8931.
[17] I. Shcherbakova, S. Mitra, Hydroxyl-radical footprinting to probe equilibrium changes in RNA tertiary structure, Methods Enzymol. 468 (2009) 31–46.
[18] R. Fraczkiewicz, W. Braun, Exact and efficient analytical calculation of the accessible surface areas and their gradients for macromolecules, J. Comp. Chem. 19 (1998) 319–333.
[19] E. Menichelli, C. Isel, C. Oubridge, K. Nagai, Protein-induced conformational changes of RNA during the assembly of human signal recognition particle, J. Mol. Biol. 367 (2007) 187–203.
[20] S. Mitra, A. Laederach, B.L. Golden, R.B. Altman, M. Brenowitz, RNA molecules with conserved catalytic cores but variable peripheries fold along unique energetically optimized pathways, RNA 17 (2011) 1589–1603.
[21] M. Brenowitz, D.F. Senear, M.A. Shea, G.K. Ackers, Quantitative DNase footprint titration: a method for studying protein-DNA interactions, Methods Enzymol. 130 (1986) 132–181.
[22] D.W. Celander, T.R. Cech, Visualizing the higher order folding of a catalytic RNA molecule, Science 251 (1991) 401–407.
[23] E. Mateo-Martí, C. Briones, C. Rogero, C. Gomez-Navarro, C. Methivier, C.M. Pradier, J.A. Martín-Gago, Nucleic acid interactions with pyrite surfaces, Chem. Phys. 352 (2008) 11–18.
[24] S. Keiper, D. Bebenroth, B. Seelig, E. Westhof, A. Jaschke, Architecture of a Diels–Alderase ribozyme with a preformed catalytic pocket, Chem. Biol. 11 (2004) 1217–1227.
[25] S. Kraut, D. Bebenroth, A. Nierth, A.Y. Kobitski, G.U. Nienhaus, A. Jaschke, Three critical hydrogen bonds determine the catalytic activity of the Diels–Alderase ribozyme, Nucleic Acids Res. 40 (2012) 1318–1330.
[26] A.Y. Kobitski, A. Nierth, M. Helm, A. Jaschke, G.U. Nienhaus, Mg2+-dependent folding of a Diels–Alderase ribozyme probed by single-molecule FRET analysis, Nucleic Acids Res. 35 (2007) 2047–2059.
[27] V. Manoharan, B. Furtig, A. Jaschke, H. Schwalbe, Metal-induced folding of Diels–Alderase ribozymes studied by static and time-resolved NMR spectroscopy, J. Am. Chem. Soc. 131 (2009) 6261–6270.
[28] T. Berezniak, M. Zahran, P. Imhof, A. Jaschke, J.C. Smith, Magnesium-dependent active-site conformational selection in the Diels–Alderase ribozyme, J. Am. Chem. Soc. 132 (2010) 12587–12596.
[29] T. Berezniak, A. Jaschke, J.C. Smith, P. Imhof, Stereoselection in the Diels–Alderase ribozyme: a molecular dynamics study, J. Comput. Chem. 33 (2012) 1603–1614.